NANO LETTERS

2007
Vol. 7, No. 2
433−438

Chemical Control of Photoexcited States in Titanate Nanostructures

Alexander Riss,[†] Thomas Berger,[†] Hinrich Grothe,[†] Johannes Bernardi,[‡] Oliver Diwald,*[,†] and Erich Knözinger[†]

Institute of Materials Chemistry, Vienna University of Technology, Veterinärplatz 1/GA, A-1210 Vienna, Austria, and University Service Centre for Transmission Electron Microscopy, Vienna University of Technology, Wiedner Hauptstrasse 8-10/137, A-1040 Vienna, Austria

Received November 18, 2006

ABSTRACT

The photoelectronic properties of layered titanate nanostructures can be adjusted by changing the nature and bonding state of ions in the interlayer region. We studied the optical properties of titanate nanowires and nanotubes obtained after soft-chemical treatment of TiO_2 anatase powders. A photoluminescence emission process originating from exciton states trapped in $[TiO_6]$ units was observed in anatase TiO_2 and, with significantly enhanced intensity, in nanowires made of titanate nanosheets. On the basis of a correlation between emission intensity and the concentration of intercalated alkali ions, we conclude that protonation of the $[TiO_6]$ octahedra that constitute the titanate sheet structure suppresses radiative deactivation of trapped excitons and can be reversed by ion exchange.

Oxide nanotubes, wires, and rods constitute a promising new class of materials having uniform dimensions and well-developed morphologies.[1] In particular, TiO_2-based nanotubes and wires have attracted much attention because of a broad spectrum of potential applications: with lengths of several hundreds of nanometers, they show superior electron transport properties in dye-sensitized solar cells.[2,3] Furthermore, highly ordered nanotube arrays photocleave water into hydrogen and oxygen with higher rates compared to other titania-based devices.[4] Also, for electrochemical applications such as in sensors and batteries, titanate nanostructures are of considerable interest: their morphology was found to be beneficial for the electrochemical insertion and extraction of Li^+ ions, which gives rise to enhanced discharge rates under high reversibility.[5] As a support matrix for proteins, these materials show potential for a new generation of biosensors.[6] Last but not least, laser action and photoluminescence-related applications have been put forward because strong photoluminescence emission in the visible light region has been observed.[7−10] All of these applications have in common that TiO_2-based nanostructures provide a confined solid medium where charged species, holes, and electrons—either photogenerated within the bulk or injected from adsorbed species—can migrate, can recombine, or can finally leave the structure in the course of a surface reaction. Consequently, the nature and location of charge-trapping sites and recombination centers are critical to the rational improvement of device efficiencies and, for this reason, have to be identified.

A major advantage of TiO_2-based nanostructures is their easy and cheap production.[11] Since the first reports on the successful synthesis of titanate nanotubes,[12] extensive research has been carried out to identify their structure and to elucidate the underlying formation mechanism. Through the soft-chemistry route, bulk titanates exfoliate into monolayer sheets that are composed of edge-sharing $[TiO_6]$ octahedra.[13] Assembled as multilayers, these nanosheets provide the structural basis for both massive titanate nanowires as well as hollow titanate nanotubes. As a consequence of their size, titanate nanostructures are surface-determined materials and scroll-up into tubes is induced by changes of the solvent's pH.[14−17]

For a rational description of the optical properties of titanate nanowires and nanotubes, it is necessary to (a) compare them with those of the precursor material and (b) carefully address their variation in the course of chemistry-induced structure and morphology changes.

The transmission electron micrograph in Figure 1a characterizes the TiO_2 precursor material (Alfa Aesar no. 36199) consisting of anatase particles with diameters up to 300 nm. After 48 h of reflux treatment in an aqueous solution of 10 N NaOH ($T = 380$ K),[12,18] the precursor material is completely converted into wires (Figure 1b and c). With lengths of several hundred nanometers, these nanowires are massive

* Corresponding author. E-mail: odiwald@mail.zserv.tuwien.ac.at. Phone: 011 431 250773810. Fax: 011 431 250773890.
[†] Institute of Materials Chemistry, Vienna University of Technology.
[‡] University Service Centre for Transmission Electron Microscopy, Vienna University of Technology.

10.1021/nl062699y CCC: $37.00
Published on Web 01/17/2007

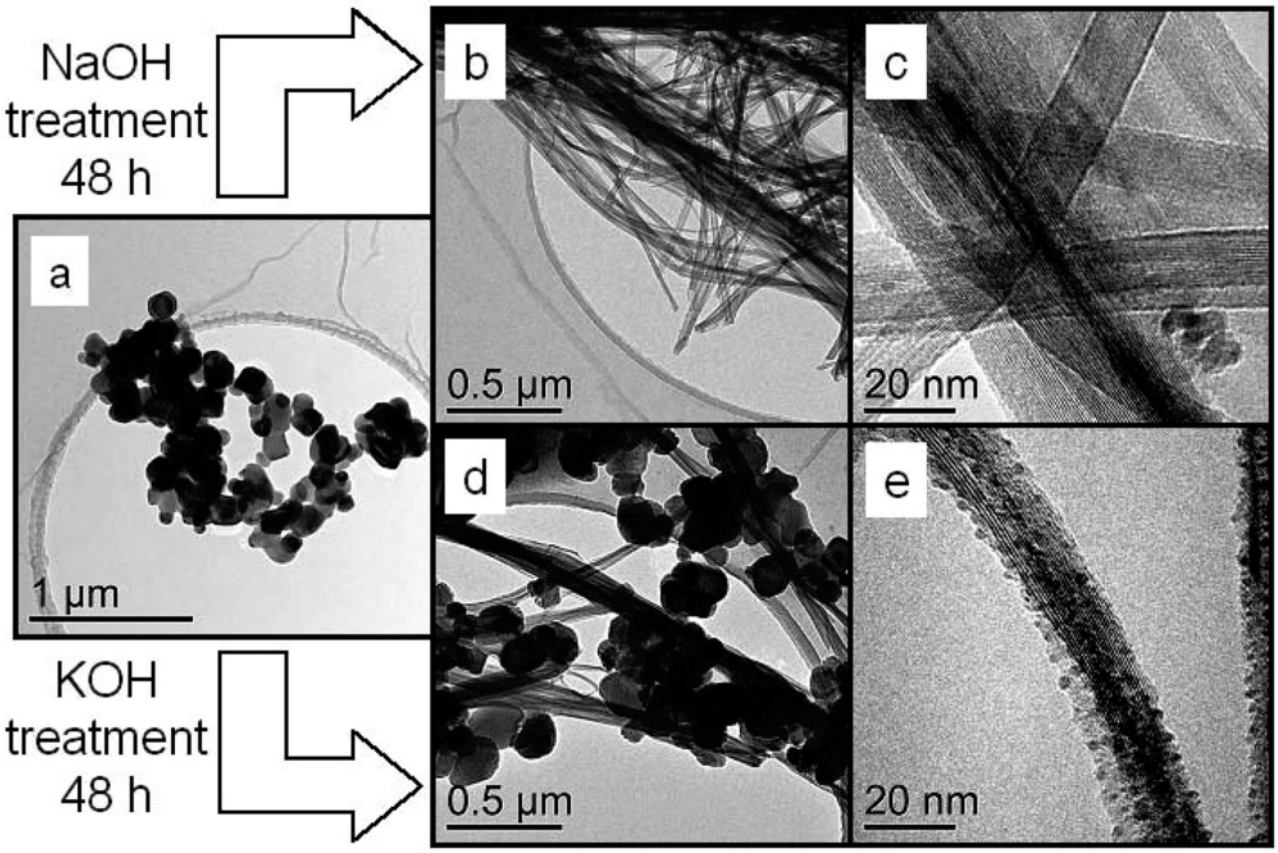

Figure 1. TEM images of commercial TiO_2 anatase grains (a) that were treated in alkaline aqueous solutions under reflux ($T = 380$ K) for 48 h (b−d). The images in parts 1b and c characterize the product after 48 h in 10 N NaOH solution, whereas parts d and e illustrate the corresponding situation when KOH was used instead of NaOH as a base. A TECNAI F20 analytical transmission electron microscope equipped with a field emission source and a S-Twin objective lens was used. Images were recorded with a Gatan 794 Multiscan camera.

and have diameters between 10 and 100 nm. A typical high-resolution image in Figure 1c reveals their relatively smooth surfaces. Parallel-oriented fringes indicate a layered structure with interlayer spacings of 7.5 ± 0.7 Å consistent with d_{020} spacings of titanate structures reported by others.[16] The situation was different when the same treatment ($t = 48$ h) was carried out with KOH instead of NaOH as the base (Figure 1d and e): only a fraction of the precursor material was transformed into wires of significantly larger diameters. A closer look at a comparatively thin wire that provides sufficient transparency for electrons for high resolution is given in Figure 1e and reveals a layered structure with spacings identical to those observed for Na-titanates (Figure 1c). The KOH-derived wires are homogeneously covered with small particles, the chemical nature of which remains unidentified so far.

Raman spectroscopy was employed for further structural characterization of the materials. The spectrum of the TiO_2 precursor in Figure 2a shows lattice vibrations at 399, 519, and 639 cm^{-1} characteristic for anatase.[19] In contrast, the NaOH-treated sample (images in Figure 1b and c) lacks these bands and shows others at 273 and 288 cm^{-1} as well as bands at 445, 660, 701, and 904 cm^{-1} (Figure 2b). All of them are consistent with the Raman data reported for titanate sheets.[20] However, the Raman spectrum of a sample that was treated for 48 h in an aqueous KOH solution contains, in addition

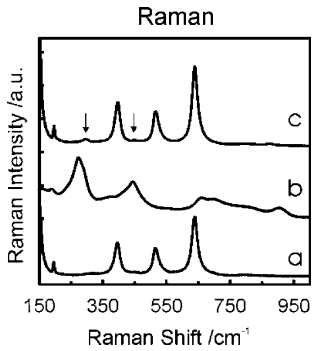

Figure 2. Raman spectra of (a) TiO_2 anatase grains, (b) Na-titanate, and (c) a mixture of K-titanate and the TiO_2 anatase precursor. The spectra were obtained with a Raman microscope system (Horiba Jobin Yvon, LabRAM HR) using a He−Ne laser (632.8 nm) for excitation. The Raman-scattered light was collected at 180°, dispersed by an optical grid and detected by a CCD camera with a spectral resolution of 4 cm^{-1}.

to the anatase-related bands, two small features (indicated by arrows in Figure 2c) attributed to the presence of K-titanate.[21] This is consistent with TEM (Figure 1d), which reveals that only a small fraction of anatase was transformed into K-titanate nanowires after 48 h.

The UV diffuse reflectance spectra of TiO_2 anatase, as well as that of the NaOH- and KOH-treated samples (see TEM images in Figures 1b and d, respectively) were found

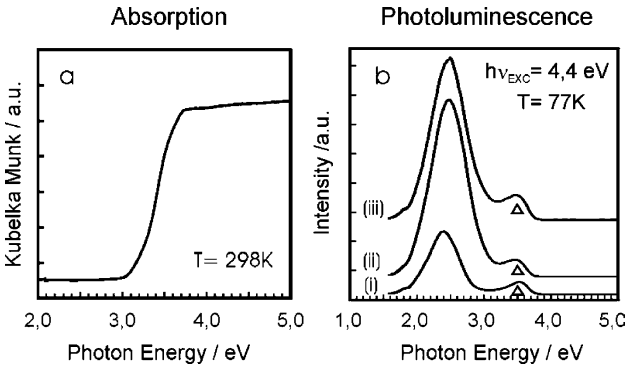

Figure 3. Optical properties of TiO_2 anatase particles and derived titanate nanostructures. (a) UV diffuse reflectance spectrum of nanostructured Na-titanate acquired at room temperature and (b) photoluminescence emission spectra of TiO_2 anatase (i), nanostructured Na-titanate (ii), and K-titanate (iii), which were measured at 77 K using 4.4 eV excitation light. The emission spectra were not normalized with respect to comparable powder densities in the optical cell. Because the powder density of the precursor material (curve i) was twice as high as those related to the titanate nanostructures the band of the normalized spectrum i would show half of the intensity plotted. The small feature indicated by a triangle corresponds to an artifact that arises from scattering effects.

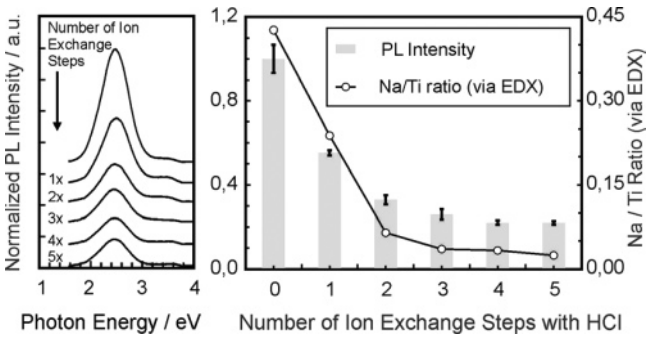

Figure 4. Photoluminescence emission bands related to Na-titanate nanowires after production and after 1−5 ion ion exchange steps with 0.1 N HCl. The spectra were acquired at 77 K using 4.4 eV excitation light. The right-hand panel of Figure 4 shows the correlation between the intensity of the emission band at 2.4 eV and the Na/Ti ratio as measured with EDX using a JSM-T330A scanning electron microscope equipped with a SUTW energy dispersive X-ray detector.

to be identical. The absorption spectrum of the Na-titanate (Figure 3a) displays an absorption edge at 3.2 eV. Its coincidence with that of bulk anatase has been predicted by a recent theoretical study which shows that, irrespective of the nanostructure morphology (nanotubes with different numbers of walls, nanostrips, and belts), the band gap approaches the value of the related bulk material for dimensions larger than 3 nm.[22] Visible photoluminescence is observed in the anatase powder at $T = 77$ K (Figure 3b curve i). The emission band has a maximum at 2.4 eV and is detectable only at temperatures below 298 K because of thermal quenching of the underlying radiative deactivation process at this temperature. Significantly enhanced intensities for the same band were measured for both Na- and K-titanate-containing samples (Figure 3b ii and iii, respectively). Additional experiments were carried out under high vacuum conditions ($p < 10^{-5}$ mbar) in order to search for surface-related effects: no changes were observed before and after partial surface dehydration carried out by vacuum treatment at 470 K. The same is true when the experiment is carried out in the presence of molecular oxygen, which efficiently quenches surface photoluminescence effects.[23] We therefore conclude that the respective radiative deactivation step occurs in the bulk and does not respond to changes at the surface despite the high surface-to-volume ratio of the material.

Treatment of layered titanate nanostructures with HCl and subsequent washing with deionized water causes sodium ion replacement by protons and can be tracked by photoluminescence measurements as well. Figure 4 (left panel) shows the photoluminescence emission spectrum of the as-produced sample (directly after alkaline treatment) in comparison to those of samples that were subjected to 1−5 steps of HCl treatment.[24] Clearly, the intensity of the emission band decreases with the number of ion exchange steps and a correlation between the integral band intensity and the alkali/titanium ratio is demonstrated for Na-titanate in the right-hand panel of Figure 4.

Alkali ion exchange against protons for sodium ions has, apart from changes in photoluminescence emission, another spectacular effect on the sample properties: it transforms massive nanowires into tubes.[11,14,15] A transmission electron micrograph of a sample that was subjected to one ion exchange step is shown in Figure 5a.[24] One can clearly observe two qualitatively different nanostructures. Although the major fraction consists of massive nanowires (Figure 1b and c), a minor one—marked with an arrow in Figure 5a—has already been transformed into nanotubes. A sample that was subjected to five ion exchange steps has been completely transformed into nanotubes having uniform inner and outer diameters of about 4 and 10 nm, respectively. Their lengths range from 50 to several hundred nanometers. HRTEM images (Figure 5b) reveal that the tubes exhibit a layered structure identical to that of the massive titanate nanowires (Figure 1c and d) and are open at both ends. Raman spectra obtained on proton-exchanged samples (not shown) show the same bands as those observed for Na^+ titanate nanowires (Figure 2b). We therefore conclude that titanate nanosheets remain the building block irrespective of morphology changes induced by their protonation.

Subsequent contact of protonated titanate nanotubes with a NaOH or KOH solution replaces protons by alkali ions and yields unscrolled titanate sheets.[11,12,14,15] This process and in particular its reversibility can be tracked by photoluminescence spectroscopy as well. Figure 6 shows the emission spectra of Na-titanate (a) after production, (b) after multiple ion exchange steps using 0.1 N HCl, and (c) after one re-exchange step in aqueous NaOH solution (10 N). As a consequence of HCl treatment, the intensity of the emission band at 2.4 eV has decreased to one-fifth of its initial value (Figure 6b). One re-exchange step at room temperature using an aqueous NaOH solution (Figure 6b) almost restores the intensity of the emission band (Figure 6c) to its initial value (Figure 6a).

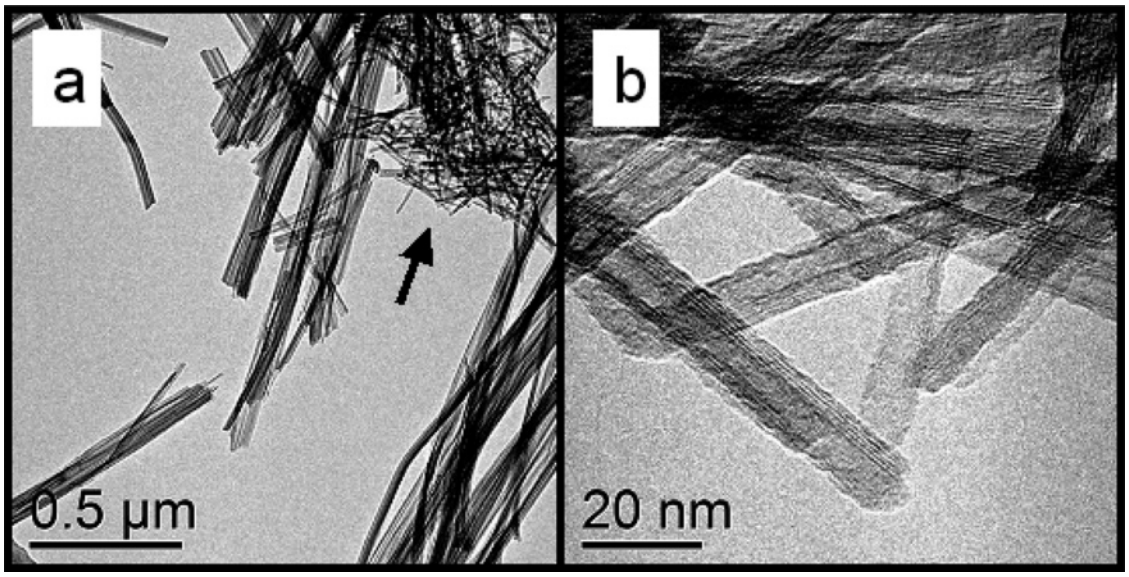

Figure 5. TEM images of titanate nanostructures (a) after one ion exchange step and (b) after five ion exchange steps with 0.1 N HCl. Two different material qualities can clearly be deduced from Figure 5a (massive titanate nanowires, on one hand, and titanate nanotubes indicated by an arrow, on the other). Figure 5b corresponds to a typical micrograph of the material after complete conversion into tubes.

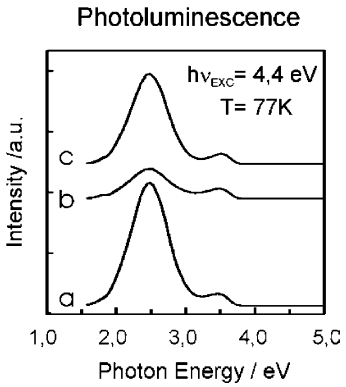

Figure 6. Photoluminescence emission of (a) Na-Titanate, (b) the material after 5 iterations of HCl treatment (bottom spectrum in Figure 4a), and (c) after one re-exchange step with NaOH. The HCl-induced decrease of photoluminescence intensity is almost reobtained after subsequent NaOH treatment.

On TiO_2 and various titanates, visible luminescence emission around 2.4 eV has been reported by different groups and has uniformly been attributed to an electronic transition that is associated with the $[TiO_6]$ octahedron as the basic structural unit and therefore of very local character.[25−28] In TiO_2, two competing emission processes can result from photoexcitation.[29] One is characterized by exciton localization where the excited state induces local distortion of the $[TiO_6]$ octahedron. The energy of such trapped exciton states is lowered by the amount of lattice relaxation energy.[30] A second process is based on intersite exciton transfer and gives rise to free exciton emission. The excitonic properties of TiO_2-based materials depend on the particular environment of the $[TiO_6]$ octahedron, that is, its coordination state within the crystal structure. In rutile as the more dense structure, the $[TiO_6]$ octahedron has a higher coordination number (cn = 10) than in anatase (cn = 8) or in the related titanates (cn ≤8) and, concomitantly, free exciton emission prevails.[31] Support for the existence of trapped excitons in anatase and their absence in rutile stems from optical absorption studies on TiO_2 single crystals: in contrast to rutile, the Urbach-type behavior of the fundamental absorption edge of anatase indicates exciton localization mediated by phonon interaction.[31]

On the basis of the above-mentioned studies and the fact that the 2.4 eV emission is observed in the anatase precursor material as well as in Na- and K-containing titanates, we ascribe the respective emission to the radiative deactivation of excitons trapped within the $[TiO_6]$ units. A closer look at the atomic structure of the titanate nanosheets is helpful to rationalize why the exchange of intercalated alkali ions (Na^+ or K^+) with protons leads to substantial depletion of photoluminescence emission. Zhang et al. investigated the relaxed atomic configurations of $Na_2Ti_3O_7$ and $H_2Ti_3O_7$.[32] Both structures are made of $[TiO_6]$ octahedra with shared edges and corners (Figure 7).

The positions and bonding states of alkali ions and protons, however, are very different. Na^+ being placed in the middle between the titanate layers has a distance of more than 2 Å from the next oxygen ion. Therefore, alkali ions located between the negatively charged titanate sheets are weakly bonded and represent mobile species. Conversely, the distance between a proton and an octahedral oxygen ion is with 1 Å significantly shorter and implies chemical bonding. Furthermore, theory predicts that protonation of the $[TiO_6]$ unit partially transfers electron density from the Ti−O moiety to the O−H bond and causes the increase of an adjacent Ti−O bond length.[32] The resulting structural distortion of the protonated octahedron (right-hand side of Figure 7) is proposed to change the potential energy surface in such a way that the excited state does not localize inside $[TiO_6]$ anymore and photoluminescence emission does not appear. Alkali ion insertion into the interlayer region induces

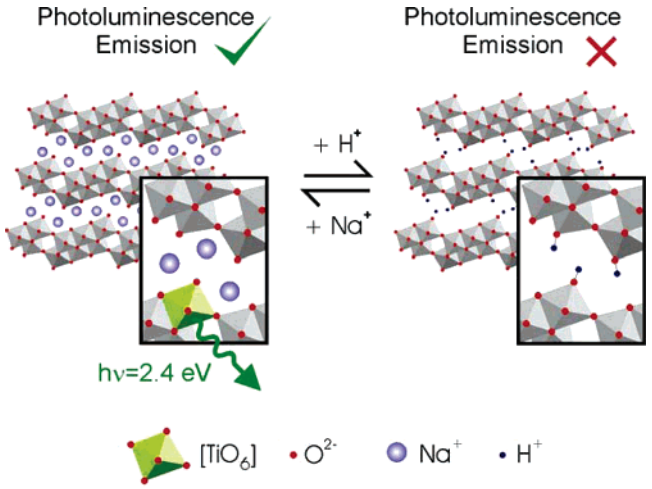

Figure 7. Scheme of reversible ion exchange within layered titanate nanostructures as adapted from ref 32. In contrast to intercalated Na^+ ions, which are weakly bonded, chemisorbed protons lead to a distortion of the $[TiO_6]$ octahedron, related to the reduction of trapped exciton deactivation (see text).

deprotonation and restores the original electronic and geometric structure of the $[TiO_6]$ octahedron. As a result, an excited state having a sufficiently long lifetime to luminesce can be formed.

Essentially, three processes stand in competition with the chemical utilization of photogenerated charges in TiO_2-based materials: (i) radiative and (ii) nonradiative recombination of charge carriers as well as (iii) charge trapping at specific surface or bulk defects.[33] Such trapped charge carriers that are currently under investigation in our lab can recombine at some later stage, but, in principle, remain separated and thus chemically active at first run. The branching ratio between these key processes has to be controlled in order to optimize the desired functionality of the titanate-based device. The fact that trapped exciton states are directly linked to the presence of alkali ions within the titanate structure in addition to the fact that ion exchange can be accomplished easily by soft-chemical treatment carries twofold technological potential: First, ion exchange can be monitored directly by photoluminescence measurements and, thus, provides a basis for sensing the composition of the interlayer region between the titanate nanosheets. Second, the intensity of photoluminescence emission is adjustable by chemical treatment and allows for chemical control over the photoelectronic properties of uniformly sized and morphologically well-defined nanostructures.

In conclusion, we have shown that facile ion exchange in titanate nanostructures (thus the deliberate increase or depletion of certain ions within the interlayer region) controls their photoelectronic properties. The accessibility of the interlayer region for various ions opens an efficient path for the controlled chemical modification of the $[TiO_6]$ subunit, the electronic details of which depend on their particular environment. Protonation of octahedral oxygen ions suppresses the radiative deactivation of trapped excitons. However, the process can reversibly be reinforced by back-exchange with alkali ions that bind only weakly to these units. These results are not only important for photocatalytic and electrochemical applications that are limited by charge-carrier recombination. They also open up synthetic venues for the chemical control of photoelectronic properties of layered oxide-based nanostructures.

Acknowledgment. This work was financially supported by the Fonds zur Förderung der Wissenschaftlichen Forschung (FWF − P17514-N11), which is gratefully acknowledged. Raman measurements were rendered possible by the TU Vienna grant “innovative project 2003”. We thank P.V. Sushko for very useful discussions and his critical comments on the manuscript.

References

(1) Patzke, G. R.; Krumeich, F.; Nesper, R. *Angew. Chem., Int. Ed.* **2002**, *41*, 2446.
(2) Ohsaki, Y.; Masaki, N.; Kitamura, T.; Wada, Y.; Okamoto, T.; Sekino, T.; Niihara, K.; Yanagida, S. *Phys. Chem. Chem. Phys.* **2005**, *7*, 4157.
(3) Mor, G. K.; Shankar, K.; Paulose, M.; Varghese, O. K.; Grimes, C. A. *Nano Lett.* **2006**, *6*, 215.
(4) Mor, G. K.; Shankar, K.; Paulose, M.; Varghese, O. K.; Grimes, C. A. *Nano Lett.* **2005**, *5*, 191.
(5) Gao, X. P.; Lan, Y.; Zhu, H. Y.; Liu, J. W.; Ge, Y. P.; Wu, F.; Song, D. Y. *Electrochem. Solid-State Lett.* **2005**, *8*, A26.
(6) Liu, A.; Wei, M.; Honma, I.; Zhou, H. *Anal. Chem.* **2005**, *77*, 8068.
(7) (a) Quian, L.; Jin, Z.-S.; Yang, S.-Y.; Du, Z.-L.; Xu, X. R. *Chem. Mater.* **2005**, *17*, 5334. (b) Qian, L.; Jin, Z.-S.; Zhang, J.-W.; Huang, Y.-B.; Zhang, Z.-J.; Du, Z.-L. *Appl. Phys. A* **2005**, *80*, 1801.
(8) Sun, X.; Li, Y. *Chem.—Eur. J.* **2003**, *9*, 2229.
(9) Khan, M. A.; Jung, H.-T.; Yang, O.-B. *J. Phys. Chem. B* **2006**, *110*, 6626.
(10) Bavykin, D. V.; Gordeev, S. N.; Moskalenko, A. V.; Lapkin, A. A.; Walsh, F. C. *J. Phys. Chem. B* **2005**, *109*, 8565.
(11) Tsai, C.-C.; Teng, H. *Chem. Mater.* **2006**, *18*, 367.
(12) (a) Kasuga, T.; Hiramatsu, M.; Hoson, A.; Sekino, T.; Niihara, K. *Langmuir*, **1998**, *14*, 3160. (b) Kasuga, T.; Hiramatsu, M.; Hoson, A.; Sekino, T.; Niihara, K. *Adv. Mater.* **1999**, *11*, 1307.
(13) Orzali, T.; Casarin, M.; Granozzi, G.; Sambi, M.; Vittadini, A. *Phys. Rev. Lett.* **2006**, *97*, 156101.
(14) Saponjic, Z. V.; Dimitrijevic, N. M.; Tiede, D. M.; Goshe, A. J.; Zuo, X.; Chen, L. X.; Barnard, A. S.; Zapol, P.; Curtiss, L.; Raijh, T. *Adv. Mater.* **2005**, *17*, 965.
(15) Barnard, A.; Saponjic, Z.; Tiede, D.; Rajh, T.; Curtiss, L. *Rev. Adv. Mater. Sci.* **2005**, *10*, 21.
(16) Mao, Y.; Wong, S. S. *J. Am. Chem. Soc.* **2006**, *128*, 8217.
(17) Banard, A. S.; Curtiss, L. A. *Nano Lett.* **2005**, *5*, 1261.
(18) Yang, J.; Jin, Z.; Wang, X.; Li, W.; Zhang, J.; Zhang, S.; Guo, X.; Zhang, Z. *Dalton Trans.* **2003**, *20*, 3898.
(19) Ohsaka, T.; Izumi, F.; Fujiki, Y. *J. Raman Spectrosc.* **1978**, *7*, 321.
(20) Ma, R.; Fukuda, K.; Sasaki, T.; Osada, M.; Bando, Y. *J. Phys. Chem. B* **2005**, *109*, 6210.
(21) The shift between Na-titanate- and K-titanate-related bands is attributed to slightly different potentials induced by interlayer Na^+ and K^+ ions, respectively.
(22) Enyashin, A. N.; Seifert, G. *Phys. Status Solidi B* **2005**, *242*, 1361.
(23) Stankic, S.; Sterrer, M.; Hofmann, P.; Bernardi, J.; Diwald, O.; Knözinger, E. *Nano Lett.* **2005**, *5*, 1889.
(24) A typical procedure for HCl treatment involves dispersion of the material in 0.1 N HCl for 30 min, followed by centrifugation and washing of the precipitate with water. Drying of the white powder in air was applied thereafter.
(25) Tang, H.; Berger, H.; Schmid, P. E.; Lévy, F.; Burri, G. *Solid State Commun.* **1992**, *84*, 349.
(26) Mochizuki, S.; Fujishiro, F.; Minami, S. *J. Phys. C: Solid State Phys.* **2005**, *17*, 923.
(27) (a) Sekiya, T.; Tasaki, M.; Wakabayashi, K.; Kurita, S. *J. Lumin.* **2004**, *108*, 69. (b) Wakabayashi, K.; Yamaguchi, Y.; Sekiya, T.; Kurita, S. *J. Lumin.* **2005**, *112*, 50.
(28) De Haart, L. G. J.; De Vries, A. J.; Blasse, G. *J. Solid State Chem.* **1985**, *59*, 291.

(29) Toyozawa, Y. *J. Lumin.* **1976**, *12/13*, 13.
(30) Song, K. S.; Williams, R. T. *Self-Trapped Excitons*, 2nd ed; Springer: Berlin, 1996; Vol. 105.
(31) Tang, H.; Lévy, F.; Berger, H.; Schmid, P. E. *Phys. Rev. B* **1995**, *52*, 7771.
(32) Zhang, S.; Chen, Q.; Peng, L.-M. *Phys. Rev. B* **2005**, *71*, 014104.
(33) (a) Berger, T.; Sterrer, M.; Diwald, O.; Knözinger, E.; Yates, J. T., Jr. *Phys. Chem. Chem. Phys.* **2006**, *8*, 1822. (b) Berger, T.; Sterrer, M.; Diwald, O.; Knözinger, E. *Chem. Phys. Chem.* **2005**, *6*, 2104.

NL062699Y